Structural Engineering and Mechanics, *Vol. 71, No. 1 (2019) 45-56*
DOI: https://doi.org/10.12989/sem.2019.71.1.045

Seismic behavior enhancement of frame structure considering parameter sensitivity of self-centering braces

Longhe Xu*[1], Xingsi Xie[1], Xintong Yan[1] and Zhongxian Li[2]

[1]*School of Civil Engineering, Beijing Jiaotong University, Beijing 100044, China*
[2]*Key Laboratory of Coast Civil Structure Safety of China Ministry of Education, Tianjin University, Tianjin 300072, China*

(Received December 8, 2018, Revised February 26, 2019, Accepted March 20, 2019)

Abstract. A modified mechanical model of pre-pressed spring self-centering energy dissipation (PS-SCED) brace is proposed, and the hysteresis band is distinguished by the indication of relevant state variables. The MDOF frame system equipped with the braces is formulated in an incremental form of linear acceleration method. A multi-objective genetic algorithm (GA) based brace parameter optimization method is developed to obtain an optimal solution from the primary design scheme. Parameter sensitivities derived by the direct differentiation method are used to modify the change rate of parameters in the GA operator. A case study is conducted on a steel braced frame to illustrate the effect of brace parameters on node displacements, and validate the feasibility of the modified mechanical model. The optimization results and computational process information are compared among three cases of different strategies of parameter change as well. The accuracy is also verified by the calculation results of finite element model. This work can help the applications of PS-SCED brace optimization related to parameter sensitivity, and fulfill the systematic design procedure of PS-SCED brace-structure system with completed and prospective consequences.

Keywords: frame structure; genetic algorithm; parameter sensitivity analysis; structural optimization; self-centering brace

1. Introduction

With the reformation of the existing performance-based seismic design, the traditional earthquake-resilient structural systems need to be upgraded due to the high demands of limitative residual deformation which may result in the cost of structural repairs. Previous researches show that the structural repair cost will exceed its reconstruction cost once the ratio of residual deformation is higher than 0.5% (McCormick *et al.* 2008). Considering that the cumulative plastic deformation induced by the inelastic actions of components is inevitable under strong earthquakes, it is necessary to append energy dissipation and self-centering systems to retard the damage evolution of the original structures.

Various earthquake-resilient substructures have been proposed and experimentally verified. For instance, rocking systems, pre-stressing beam-column joints (Yurdakul and Avsar 2016, Zhang *et al.* 2016, Wang *et al.* 2017), self-centering systems (Rojas *et al.* 2009, Guerrini *et al.* 2014, Henry *et al.* 2016, Xu *et al.* 2016a) and self-centering braces (Erochko *et al.* 2013, Chou and Chung 2014) are all efficient components for energy dissipation and recentering capability improvement. Seismic analyses and hysteretic behavior studies have shown that structures employing self-centering braces have smaller residual deformation than structures using buckling-restrained braces alone (Marshall and Charney 2012). In order to enhance the seismic behavior of the brace-structure system, one of the complex and coupled problems, the optimum locations of these devices and the corresponding design parameters, should be presupposed before the other one is initiated in general.

For current brace-structure system, engineers usually select the brace design parameters first, and gradually optimize them to obtain the relatively optimal brace-structure design results, mostly relying on personal experience. This will sometimes lead to unreasonable brace-structure system design. Nowadays, researchers advocate more precise and scientific optimization methods. An optimization process requires optimized objective, optimization algorithm and specific measures. Considering that the difficulty of parameters analyses increases with the expansion of the parameter domain (both quantity and range), an appropriate optimization algorithm can greatly improve the computational convergence and reduce computation time. Based on numerous mathematical models, a large number of optimization algorithms have been developed and applied to the design and verification of structures, such as harmony search algorithm (Degertekin and Hayalioglu 2010), teaching-learning-based optimization algorithm (Dede and Ayvaz 2013), chaotic artificial bee colony algorithm (Xu *et al.* 2015), collaborative-climb monkey algorithm (Yi *et al.* 2015), and so on. Recently, genetic algorithm (GA) has been gradually used for structural parameter optimization (Liu *et al.* 2010, Rojas *et al.* 2011, Abbasnia *et al.* 2014). Losanno *et al.* (2015) proposed a solution to a design optimization problem for a simple linear-elastic one-bay one-story frame equipped with elastic-deformable viscous or friction dissipative braces.

*Corresponding author, Ph.D., Professor
E-mail: lhxu@bjtu.edu.cn

Copyright © 2019 Techno-Press, Ltd.
http://www.techno-press.com/journals/sem&subpage=7
ISSN: 1225-4568 (Print), 1598-6217 (Online)

They also provided an exhaustive treatment for the analysis of non-proportional damping structures (Losanno *et al.* 2017a), as well as defined optimal design parameters characterizing the isolation system of a bridge (Losanno *et al.* 2014). However, as a stochastic algorithm with multiple iterative requirements, the analysis of the influence of essential build-in parameters on the optimization process and the results seems to be inefficient and non-universal. Therefore, a response-dependent optimization method should be proposed to constantly redress the route towards the local optimal solution from another perspective.

In this paper, the formula of piecewise mechanical model is updated to simulate the seismic responses, regarding a new type of pre-pressed spring self-centering energy dissipation (PS-SCED) brace proposed by Xu *et al.* (2016a, b) as an object. The linear acceleration method based modelling of brace-structure system is developed as well. In addition, the response sensitivities of brace parameters are presented to analyze the effect of these homologous parameters on the predicted response quantities. Moreover, a GA based PS-SCED brace-structure optimization for frame considering the sensitivity of brace parameters is carried out to improve the algorithm convergence and general optimized results.

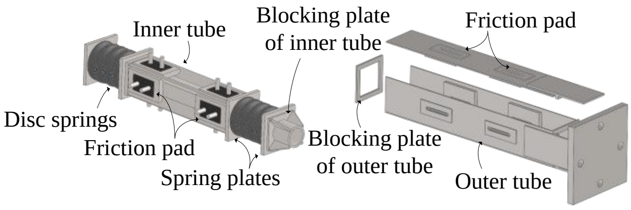

Fig. 1 Schematic drawing of PS-SCED brace

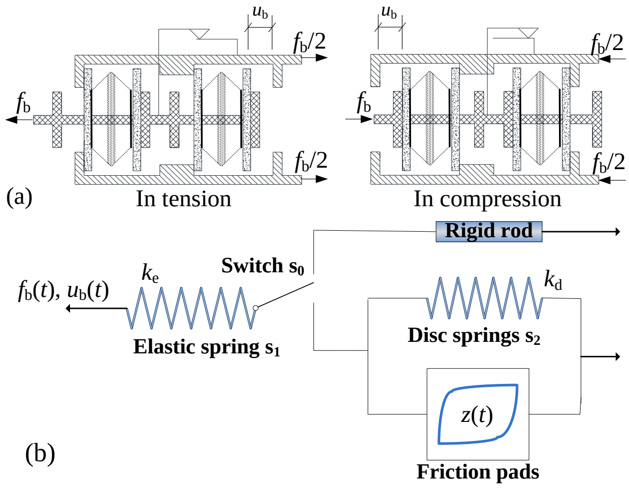

Fig. 2 (a) Working principle and (b) rheological model of PS-SCED brace

2. Response analysis of brace-structure system

2.1 Explicit time-discrete formula of PS-SCED brace

The schematic drawing of a typical PS-SCED brace is shown in Fig. 1. During the relative movement between the inner and outer tubes, an adequate energy dissipation is added by the Coulomb friction devices. The pre-pressed disc springs, the spring plates, and the blocking plates constitute the recentering device of the brace. The disc springs are always compressed. When the restoring force exceeds the activation force of the brace, the inner and outer tubes move relatively. When the displacement reaches its maximum level and then begins to decrease, its restoring force immediately reduces by twice as much as the friction force, while there is no relative movement between the inner and outer tubes, as shown in Fig. 2(a). Before activation (when the force of brace is less than the sum of the friction force and pre-pressed force), the behavior of the PS-SCED brace is reproduced by a rheological model where an elastic spring s_1 with a stiffness k_e (represents the combined stiffness of the inner and outer tubes of the brace) is connected in series with a rigid rod by a switch s_0, as shown in Fig. 2(b). Once the brace is activated, s_0 is switched to the other side, and s_1 is connected in series with the paralleling of friction pads exhibiting a Bouc-Wen hysteresis variable $z(t)$ (Ismail *et al.* 2009) and disc springs s_2 with a stiffness k_d. Although the original restoring force model can accurately simulate the behavior of brace under experimental loading schemes, due to the lack of an indication of relevant state variable S, the distortion occurs when the working stage of the brace is misjudged under the random seismic inputs. So a revised evolution law is derived as,

$$S=\begin{cases} S+1 & ,S=0 \text{ and } u_b(t_n)u_b(t_{n-1})\le 0 \\ S-1 & ,S=1 \text{ and } u_b(t_n)>d_0 \\ S & ,\text{else} \end{cases} \tag{1}$$

$$f_b(t_n)=\begin{cases} k_e u_b(t_n) & ,S=1 \\ k_e d_0 z(t_n)\dfrac{F_0}{F_0+P_0}+\text{sgn}(u_b(t_n))P_0 & \\ +k_d u_b(t_n)-k_d d_0\,\text{sgn}(u_b(t_n)) & ,\text{else} \end{cases} \tag{2}$$

where the original value of S is 0 and $f_b(t_n)$ is the restoring force of the brace at time step n; $u_b(t_n)$ and $u_b(t_{n-1})$ are the relative displacements between two ends of the brace at time step n and n-1, respectively; F_0 is the Coulomb friction force of the friction pads and P_0 is the pre-pressed force of the springs s_2. The yield displacement is $d_0=(F_0+P_0)/k_e$, and sgn( ) is the symbolic function that returns values of -1 or 1. The hysteresis variable $z(t_n)$ is expressed as,

$$\dot{z}(t_n)=\frac{1}{d_0}\left[\dot{u}_b(t_n)-\gamma\left|\dot{u}_b(t_n)\right|z(t_n)\left|z(t_n)\right|^{\alpha-1}-\beta\dot{u}_b(t_n)\left|z(t_n)\right|^{\alpha}\right] \tag{3}$$

where β, γ and α are all non-dimensional parameters that control the hysteresis shape; $\dot{u}_b(t_n)$ is the relative velocity between two ends of the brace. $z(t_n)$ can be easily given by the classical Runge-Kutta method in the explicit time-discrete formula. It should be mentioned that the numerical differential expression of $z(t_n)$ consists of parameters β, γ and d_0 which refers to design parameters k_e, k_d, F_0 and P_0 of the PS-SCED brace.

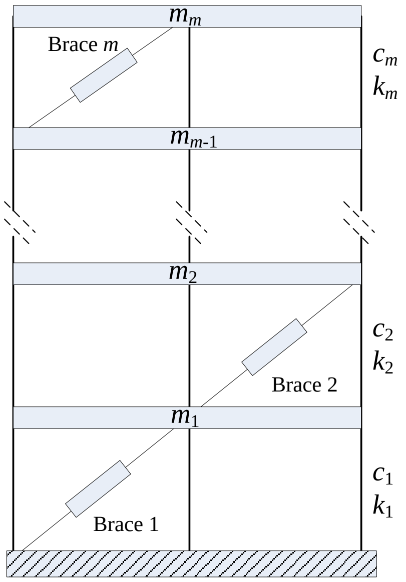

Fig. 3 MDOF model of PS-SCED brace-structure system

2.2 Brace-structure system modelling

For simplicity, the frame structure dominated by shear deformation can be simplified as multi-particle series models with a specific stiffness k_i, a mass m_i and a damping coefficient c_i of each story, as shown in Fig. 3. Note that only the horizontal stiffness contribution of the PS-SCED braces is considered and the axial stiffness of the columns is infinite regardless of the vertical vibration of the structure in this study.

Based on the restoring force model of the PS-SCED brace in Section 2.1, the dynamic responses of the m-story MDOF system can be described as follows,

$$\boldsymbol{M\ddot{u}}+\boldsymbol{C\dot{u}}+\boldsymbol{Kx}+\boldsymbol{f}_{\mathrm{b}}=-\boldsymbol{Me}\ddot{\boldsymbol{u}}_{\mathrm{g}} \tag{4}$$

where $\boldsymbol{M}$, $\boldsymbol{C}$ and $\boldsymbol{K}$ are the $m\times m$ structural mass, damping and stiffness matrices; $\boldsymbol{u}$, $\dot{\boldsymbol{u}}$ and $\ddot{\boldsymbol{u}}$ are the $m\times1$ vectors of structural displacement, velocity and acceleration; $\boldsymbol{e}$ is a $m\times1$ unity vector and $-\boldsymbol{Me}\ddot{\boldsymbol{u}}_{\mathrm{g}}$ is the external force; the $m\times1$ vector $\boldsymbol{f}_{\mathrm{b}}$ of brace restoring force is given as,

$$\boldsymbol{f}_{\mathrm{b}}=\boldsymbol{\varLambda}\boldsymbol{f}_{\mathrm{be}} \tag{5}$$

where $\boldsymbol{\varLambda}$ is the $m\times n_{\mathrm{b}}$ location matrix for the brace-structure system with respect to the masses; the $m\times1$ vector $\boldsymbol{f}_{\mathrm{be}}$ is calculated as,

$$\boldsymbol{f}_{\mathrm{be}}=\begin{pmatrix} f_{\mathrm{b1}} \\ f_{\mathrm{b2}} \\ f_{\mathrm{b3}} \\ \cdots\cdots \\ f_{\mathrm{bn_b}} \end{pmatrix}=\boldsymbol{f}_{\mathrm{b}}(\boldsymbol{\varLambda}'\boldsymbol{u},\boldsymbol{\varLambda}'\dot{\boldsymbol{u}}) \tag{6}$$

where n_{b} is the number of the braces and $\boldsymbol{\varLambda}'$ is the transposition of matrix $\boldsymbol{\varLambda}$. If each story contains one PS-SCED brace, as is the case in this study in Section 4,

$$\boldsymbol{\varLambda}=\begin{pmatrix} 1 & -1 & & \\ & 1 & -1 & \\ & & \cdots\cdots & \\ & & & 1 \end{pmatrix}_{m\times n_{\mathrm{b}}} \tag{7}$$

It is reasonable for integration of the brace restoring force at the same story, as the rigid floors ensure the compatibility of brace displacements. Note that the disassembly of the integrated brace parameters should be properly addressed in the future. Eq. (4) can be solved by the incremental form of linear acceleration method,

$$\begin{aligned}\Delta\boldsymbol{u}=&(\boldsymbol{K}+\frac{3}{\Delta t}\boldsymbol{C}+\frac{6}{\Delta t^2}\boldsymbol{M})^{-1}[\boldsymbol{M}(-\Delta\ddot{\boldsymbol{u}}_{\mathrm{g}}+\frac{6}{\Delta t}\dot{\boldsymbol{u}}_n+3\ddot{\boldsymbol{u}}_n)\\&+\boldsymbol{C}(3\dot{\boldsymbol{u}}_n+\frac{\Delta t}{2}\ddot{\boldsymbol{u}}_n)-(\boldsymbol{f}_{\mathrm{b},\,n+1}-\boldsymbol{f}_{\mathrm{b},\,n})]\end{aligned} \tag{8}$$

$$\boldsymbol{f}_{\mathrm{b},\,n+1}=\boldsymbol{\varLambda}\boldsymbol{f}(\boldsymbol{\varLambda}'\boldsymbol{u}_n,\boldsymbol{\varLambda}'\boldsymbol{u}_{n+1},\boldsymbol{\varLambda}'\dot{\boldsymbol{u}}_{n+1}) \tag{9}$$

$$\boldsymbol{u}_{n+1}=\boldsymbol{u}_n+\Delta\boldsymbol{u} \tag{10}$$

$$\dot{\boldsymbol{u}}_{n+1}=\dot{\boldsymbol{u}}_n+\Delta\dot{\boldsymbol{u}} \tag{11}$$

$$\Delta\dot{\boldsymbol{u}}=\frac{3}{\Delta t}\Delta\boldsymbol{u}-3\dot{\boldsymbol{u}}_n-\frac{\Delta t}{2}\ddot{\boldsymbol{u}}_n \tag{12}$$

where Δt is the time integration interval. The exact dynamic solution is to solve the coupled Eqs. (8)-(12) with unknown quantities $\Delta\boldsymbol{u}$ and $\boldsymbol{f}_{\mathrm{b},n+1}$. While the function $\boldsymbol{f}()$ is piecewise, considering two possible states of each brace, there are 2^n_{b} cases for this problem. Using $\boldsymbol{f}_{\mathrm{b},n+1}$ and $\boldsymbol{f}_{\mathrm{b},n}$ to calculate is hard for obtaining an unique solution of this problem, usually producing two more solutions to satisfy the qualification. Therefore, $\boldsymbol{f}_{\mathrm{b},n+1}$ and $\boldsymbol{f}_{\mathrm{b},n}$ are replaced by the values at the previous incremental step $\boldsymbol{f}_{\mathrm{b},n}$ and $\boldsymbol{f}_{\mathrm{b},n-1}$, to decouple the equations, resulting in a one-step hysteresis of brace-structure system response. When Δt is small enough, the calculation precision is within an acceptable range.

3. GA optimization and parameter sensitivity analysis

3.1 Mathematical formulation of the optimization

Although the multi-parametric effect analysis of the structural response can be given by orthogonal experiment with tremendous cases within the domain boundary, the results are still confined to special cases and bound up with the analysis procedures. In this study, an automatic brace design algorithm is used to obtain the local optimal solution of the parameters from the default values, which can be easily extended to the global optimum only if the default range is large enough. Therefore, the simplest form of the structural optimization problem is formulated as follows,

$$\min(\sum_{i=1}^{p}\eta_i a_{\mathrm{is}}) \tag{13}$$

$$\text{subject to} \begin{cases} g_j(\boldsymbol{\theta}) \geq 0, \; j = 1, \ldots, r \\ \theta_i \in R^d, \; i = 1, \ldots, q \end{cases} \tag{14}$$

$$\eta_i = \left(\frac{1}{p-1}\sum_{\substack{i=1 \\ i \neq p}}^{p} \frac{\min(a_j)}{a_{io}}\right) / \left(\sum_{i=1}^{p} \frac{\min(a_i)}{a_{io}}\right) \tag{15}$$

where Eq. (13) is the objective function to be reached and a_{is} is the ith of p prescribed performance index normalized by the initial value a_{io}. Eqs. (13) and (14) are general expressions of the minimum optimization algorithm, and the control variables and parameter fields can be selected as appropriate. η_i is the corresponding weighting coefficient which guarantees the dominance of a_{is} with a larger rate of convergence in multi-objective optimization, as shown in Eq. (15). It can be easily confirmed that the sum of η_i equals 1. $g_j(\ )$ is the jth of r deterministic constraints of the problem and $\boldsymbol{\theta}$ is the vector of q design variables that take values from a theoretically continuous set R^d.

In terms of the low expense of optimization cycles, GA is applicable for handling complex optimization problems. In general, attached to fixed length character strings, the individual genetic information directly indicates its characteristics in a population. In this study, $\boldsymbol{M}$, $\boldsymbol{K}$ and $\boldsymbol{C}$ should be firstly determined by given story mass, stiffness and damping ratio ζ. According to the site soil eigenperiod and design intensity, the seismic inputs are supposed to be appropriately selected. After stipulating the performance index and solving the dynamic equations of the brace-structure system with the default values of the brace design parameters, each a_{io} is obtained for the further researches. In general, n_{g0} is defined as the size of the initial population. A $n_{g0}\times(q\times m)$ matrix $\boldsymbol{G}$ with randomly generated integers g_{ij} is defined, where g_{ij} stands for the modification of the ith design variable by jth deterministic constraint. The designated parameter is multiplied by a coefficient of $1+c_v$ (v=1, 2,..., 5) randomly. There are n_{g0} individuals in the initial population for the brace-structure system. After eliminating the schemes that do not satisfy Eq. (14), n_{g0} is reduced to n_{g1} (the number of individuals in the first population). After solving n_{g1} dynamic equations, comparisons of Eq. (13) are conducted to filter out the optimal individual in first generation g_1, and default brace parameters are replaced at the same time. Meanwhile, to get the second generation g_2, crossover and mutation are applied to the next loop by GA operators which do not end until the pre-specified number of generations is reached, or a convergence criterion is met. The penalty of objective function is not taken into account in this study.

3.2 Optimization incorporating parameter sensitivity analysis

Even though the initial population size n_{g0}, the crossover rate r_c (to replace the partial structure of two individuals to generate a new individual) and the mutation rate r_m (to change genetic values of some individuals) in GA operator have not been discussed yet, the critical parameter c_v still has a great influence on the convergence and the optimization results. It is unreasonable to consider that different parameters are supposed to share a common change rate even with an identical random index. Therefore, the parameter sensitivity is applied in the GA operator to modify the parameter c_v. The sensitivity of response quantity $\boldsymbol{r}$ with respect to a sensitivity parameter $\boldsymbol{\theta}$ is defined as $\mathrm{d}\boldsymbol{r}/\mathrm{d}\boldsymbol{\theta}$. For a time-invariant system, after the time displacement discretization using linear acceleration method, the following sensitivity equation must be solved in the unknown $\mathrm{d}\boldsymbol{u}_{n+1}/\mathrm{d}\boldsymbol{\theta}$, as the objective function is displacement-dependent,

$$\frac{\mathrm{d}u_{n+1}}{\mathrm{d}\boldsymbol{\theta}} = \frac{\mathrm{d}\ddot{u}_{n+1}}{\mathrm{d}\boldsymbol{\theta}}\frac{\Delta t^2}{6} \tag{16}$$

$$\frac{\mathrm{d}\ddot{u}_{n+1}}{\mathrm{d}\boldsymbol{\theta}}\left(\boldsymbol{M} + \frac{1}{2}\boldsymbol{C}\Delta t + \frac{1}{6}\boldsymbol{K}\Delta t^2\right) = -\frac{\mathrm{d}\boldsymbol{f}_{n+1}}{\mathrm{d}\boldsymbol{\theta}} - \frac{\mathrm{d}\bar{\boldsymbol{u}}_{g,n+1}}{\mathrm{d}\boldsymbol{\theta}} \tag{17}$$

where $\bar{\boldsymbol{u}}_{g,n+1}$ is defined as,

$$\begin{aligned} \bar{\boldsymbol{u}}_{g,n+1} &= \boldsymbol{M}\boldsymbol{e}\ddot{\boldsymbol{u}}_{\mathrm{g},n+1} + \boldsymbol{C}\left(\dot{\boldsymbol{u}}_n + \frac{1}{2}\ddot{\boldsymbol{u}}_n\Delta t\right) \\ &\quad + \boldsymbol{K}\left(\boldsymbol{u}_n + \dot{\boldsymbol{u}}_n\Delta t + \frac{1}{3}\ddot{\boldsymbol{u}}_n\Delta t^2\right) \end{aligned} \tag{18}$$

Then the solution of the sensitivity equation requires the computation of $\mathrm{d}\boldsymbol{f}_{n+1}/\mathrm{d}\boldsymbol{\theta}$, which can be obtained from the derivation of Eq. (2). Two linear modification strategies of parameter c_v with the weighted normalized parameter sensitivity s_w given as Eq. (19) are implemented, as shown in Eqs. (20)-(23). Previous studies have shown that the weighted normalized parameter sensitivity can mitigate large variations in very small response values, generally having less interest compared with the variations of larger response values (Gu *et al.* 2014). Eq. (22) gives a way to speed up the change of parameters with larger sensitivity for the distinctions, while Eq. (23) aims at the retard of these parameter changes with larger sensitivity for synchronous effects, which are respectively denoted as case I and case II in this study. The parameter optimization with unconverted c_v is denoted as case 0 as well.

$$s_\mathrm{w}(\boldsymbol{u},\boldsymbol{\theta}) = \frac{\mathrm{d}\boldsymbol{u}}{\mathrm{d}\boldsymbol{\theta}}\frac{\boldsymbol{\theta}}{\boldsymbol{u}_{\max}}\frac{\boldsymbol{u}}{\boldsymbol{u}_{\max}} \tag{19}$$

$$s_{ij}^{\mathrm{d}} = \frac{\max(s_\mathrm{w}(\boldsymbol{u}_{\mathrm{c}(j/q)},\boldsymbol{\theta}_{\mathrm{r}(j/q)}))}{\max(s_\mathrm{w}(\boldsymbol{u}_{\mathrm{c}(j/q)},\boldsymbol{\theta}))_{\mathrm{mean}}}, \; j = 1,2,\ldots,qm \tag{20}$$

$$s_{ij}^{\mathrm{i}} = \frac{\left|\min(s_\mathrm{w}(\boldsymbol{u}_{\mathrm{c}(j/q)},\boldsymbol{\theta}_{\mathrm{r}(j/q)}))\right|}{\left|\min(s_\mathrm{w}(\boldsymbol{u}_{\mathrm{c}(j/q)},\boldsymbol{\theta}))_{\mathrm{mean}}\right|}, \; j = 1,2,\ldots,qm \tag{21}$$

$$c_v = \begin{cases} c_i \cdot (s_{ij}^{\mathrm{d}})^{w}, & \dfrac{\max(s_\mathrm{w}(\boldsymbol{u}_{\mathrm{c}(j/q)},\boldsymbol{\theta}_{\mathrm{r}(j/q)}))}{\left|\min(s_\mathrm{w}(\boldsymbol{u}_{\mathrm{c}(j/q)},\boldsymbol{\theta}_{\mathrm{r}(j/q)}))\right|} > 1 \\ c_i \cdot (s_{ij}^{\mathrm{i}})^{w}, & \text{else} \end{cases} \tag{22}$$

$$c_v = \begin{cases} c_i \cdot (s_{ij}^{\mathrm{d}})^{-w}, & \dfrac{\max(s_\mathrm{w}(\boldsymbol{u}_{\mathrm{c}(j/q)},\boldsymbol{\theta}_{\mathrm{r}(j/q)}))}{\left|\min(s_\mathrm{w}(\boldsymbol{u}_{\mathrm{c}(j/q)},\boldsymbol{\theta}_{\mathrm{r}(j/q)}))\right|} > 1 \\ c_i \cdot (s_{ij}^{\mathrm{i}})^{-w}, & \text{else} \end{cases} \tag{23}$$

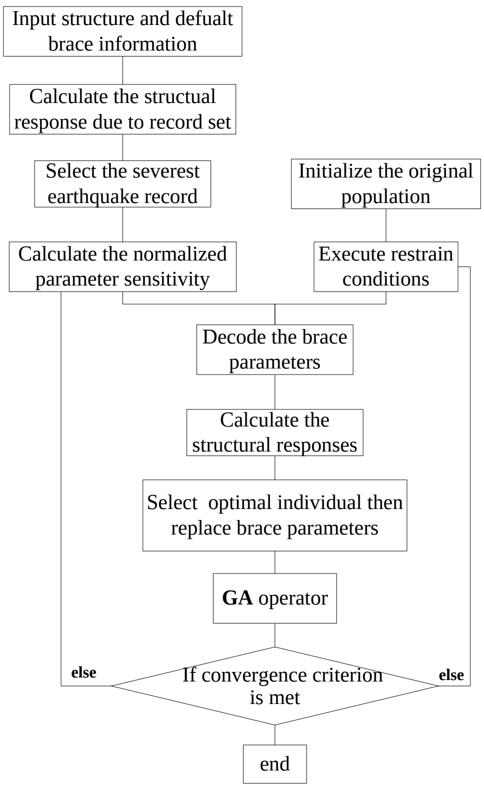

Fig. 4 Flow chart of the optimization

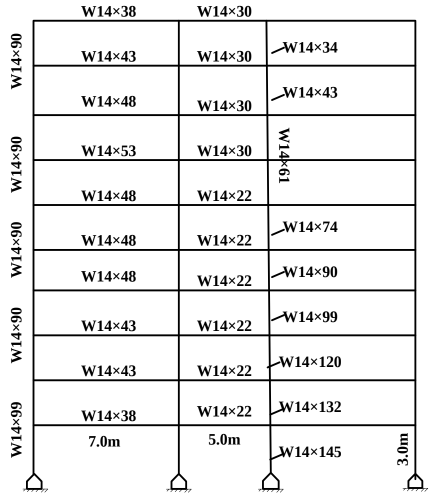

Fig. 5 Elevation of the 10-story frames (symmetric)

Table 1 Initial design parameters of PS-SCED brace and GA default parameters

PS-SCED brace	k_e /kN·m^{-1}	k_d /kN·m^{-1}	d_0/m	P_0/N	F_0/N	β	γ
	10000	1000	0.002	10000	10000	-5	6
GA	n_{g0}	r_c	r_m	c_v	w		
	1000	0.6	0.05	0.02	0.5		

where c( ) is the round up function and r( ) is the remainder function. Especially when q divides j exactly, r(j/q) equals q. The exponent w in Eqs. (22) and (23) is an index related to the convergence criterion, and the value of w should decrease as the criterion becomes more rigorous for an optimization flow without premature termination. Fig. 4 shows the flow chart of the optimization.

4. Case study

4.1 Initialization of calculation model and optimization

To verify the applicability of the proposed optimization and figure out the impacts of two forms of modified c_v on the algorithm convergence and optimization results, a 10-story 3-bay frame structure is considered as an example. The first natural period of this steel frame is 2.2 s, whose elevation arrangement is presented in Fig. 5. The mass of each story is 50 tons, and an inherent 2% Rayleigh damping in the first and second modes is used. An equivalent story stiffness study of this frame was carried out by Losanno *et al.* (2017b), so that the matrix $\boldsymbol{K}$ and $\boldsymbol{C}$ are determined as well. In this section, a_{1s} and a_{2s} are respectively the normalized maximum drift ratio and maximum roof displacement, so that p is set as 2 for this double-objective optimization problem.

To begin with, the constraint conditions of this case are formulated by the design and detailed requirements of the PS-SCED braces: (a) the stiffness ratio k_d/k_e should not exceed 0.2, as experimental studies (Xu *et al.* 2018a ,b) on this type of brace show that each k_d/k_e is no more than 0.1 while some researchers draw a conclusion that the larger k_d is, the better structural response is; (b) the force ratio F_0/P_0 should not exceed 1.3 in this case to ensure the residual deformation of PS-SCED braces within an acceptable range and guarantee the accuracy of the mechanical model; (c) $\beta+\gamma$ should be 1.0 to ensure the consistency of $z(t_n)$; (d) the individual d_0 should not exceed twice as much as its initial value, as an excessively large d_0 does not cause the activation of the brace, resulting in no additional energy dissipation during the earthquake. Because too many restrain conditions may make an over-constraint problem with few loops of optimizations, the four fundamental restrictions are enough to give full play to the advantages of adoptive algorithm.

Taking into consideration that GA is a stochastic algorithm, the convergence criterion is redefined as: the objective function of optimal individual in the kth loop is less than the mean value of the objective function of optimal individual in the (k-f_c)th to the (k-1)th loops. (f_c is an integral factor to control the convergence of the optimization, and in this case f_c equals 5.) The initial design parameters of PS-SCED brace and GA default parameters are listed in Table 1. The base shear force of the original structure under the basis ground motion is evenly distributed to each story. The braces are activated under the basis ground motion and provide no more than 75% of the lateral resisting force, as well as ensuring sufficient recentering and energy dissipation capabilities. Therefore, the initial design parameters of the braces are determined.

4.2 Optimal input of earthquake records

Since the optimization method proposed in this case is based on a certain earthquake record selected by the optimizer, considering that the earthquakes have great randomness, different ground motions have obvious impact on the optimization analysis results. In order to minimize the dispersion of earthquake randomness and preserve its inherent randomness, 22 far-field records recommended by FEMA P695 (2009) are used in this case as the basic ground motion set. Before the optimization, the responses of the original structure and brace-structure with default brace parameters under 22 ground motions are analyzed, and the severest ground motion can be selected as the earthquake input of the optimization. Each ground motion in FEMA P695 far-field record set contains two horizontal components and one vertical component. In this case, only records in two horizontal components are used as the basic inputs, so that the record set contains 44 earthquake records. The peak ground acceleration is between 0.21g and 0.82g, and the average is about 0.43g.

For small damage and easy repair after the earthquake, the design and optimization objective of the braced frame structure is that the inter-story drift ratio under the basis ground motion does not exceed the elastic limit, and the braces are activated to provide the recentering and energy dissipation capabilities. In accordance with the Code for seismic design of buildings GB50011-2010 (2016) in China, the elastic inter-story drift ratio limit of frame structure is 1/550. Although the peak ground motions (PGA) is a site specific one and commonly used, the spectral acceleration of structures corresponding to the fundamental period of structures ($Sa(T_1)$) is superior to PGA because not only $Sa(T_1)$ is a structure-specific parameter, but also the dispersion of inter-story drift ratio envelopes using $Sa(T_1)$ is obviously smaller than that using PGA. The method of $Sa(T_1)$ amplitude modulation in this case study was introduced by Ebrahimian *et al.* (2015) and Kiani and Pezeshk (2017).

Based on the results of the $Sa(T_1)$ amplitude modulation, Fig. 6 shows the inter-story drift ratio envelopes of the original structure and brace-structure with default brace parameters due to 44 ground motions. For the original structure, inter-story drift ratios under most of ground motions and their average value exceed the elastic limit. The ratios of the brace-structure are greatly reduced compared with those of the original structure, whose average value does not exceed the limit. However, under some ground motions, the drift ratios of the brace-structure still exceed the limit, wherein the ratios due to the 1999 Kocaeli earthquake in Duzce station, Turkey with the Richter scale of 7.5 are the largest. Therefore, the 1999 Kocaeli earthquake is the severest ground motion for the brace-structure with default brace parameters and is also selected as the optimization earthquake input.

4.3 Validation of parameter sensitivity

Since $z(t_n)$ is given by the classical Runge-Kutta method in the explicit time discretization formulation, the solution of $\mathrm{d}\boldsymbol{f}_{n+1}/\mathrm{d}\boldsymbol{\theta}$ may be a complicated process when $\boldsymbol{\theta}$ contains d_0, β and γ. Fortunately, d_0 can be expressed by F_0, P_0 and k_e. Besides, the shape parameters β and γ have no effect on the magnitude of the restoring force. So that only the

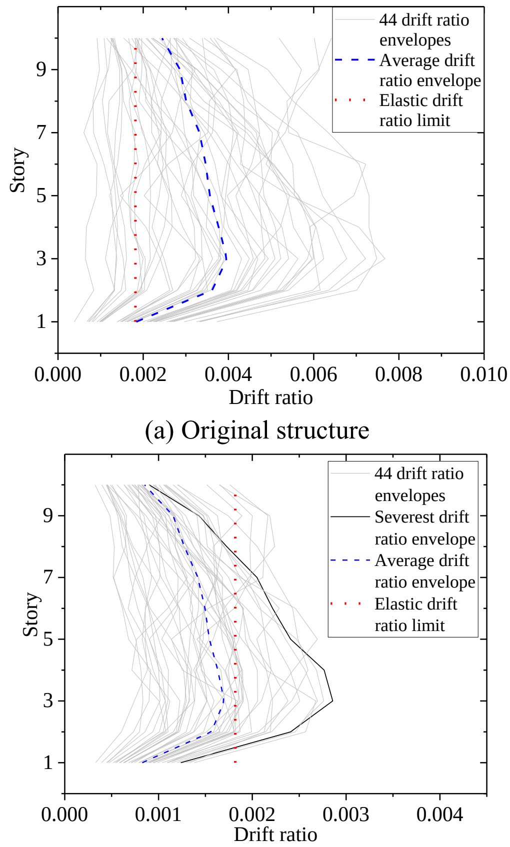

(a) Original structure

(b) Brace-structure with default brace parameters

Fig. 6 Inter-story drift ratio envelopes of the original structure and brace-structure with default brace parameters

sensitivities of the four parameters, k_e, k_d, F_0 and P_0, are considered. The evolution of the normalized response sensitivities of the first story and roof displacement to the adjacent brace parameters are shown in Figs. 7 and 8. The maximum displacements u_{max} of the first story and the roof floor are obviously different, so the value comparison between these two weighted normalized parameter sensitivities s_w is meaningless. From Fig. 7a and Fig. 8a, it is observed that the stiffness k_e has a larger influence on the node displacement vector $\boldsymbol{u}$ compared to the stiffness k_d in the first seven seconds, because there is no inter-story drift more than d_0, so the key parameter k_e directly affects the performance of the brace-structure system. The reason why the same situation comes out for pre-load P_0 is that the change of high frequency sign makes function sgn( ) magnify the effect of P_0. When the drift is greater than the yield displacement d_0, the influence of parameter F_0 and k_d is also observed, because the parameter k_d controls the stiffness sudden change of the structure and F_0 is a critical energy dissipation factor after the brace activation.

Almost all the extreme (positive and negative) values of s_w used for the modification of c_v show up when the braces are activated. A simple way to present response sensitivity is to compare these values during the earthquake, which are shown in Figs. 9 and 10. Almost every parameter sensitivity extreme value receives an inversion from positive/negative at the first floor to negative/positive at the roof. It is

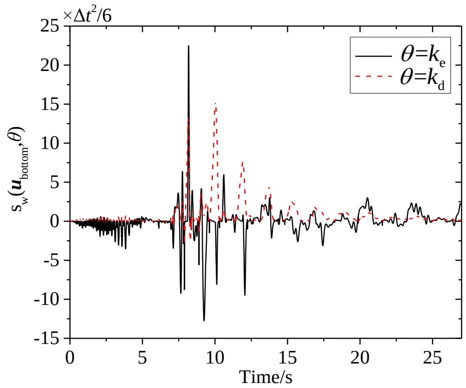

(a) Parameters k_e and k_d

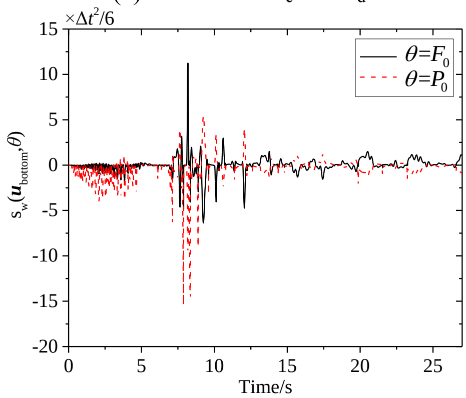

(b) Parameters F_0 and P_0

Fig. 7 Normalized response sensitivities of the first floor displacement to the adjacent brace parameters

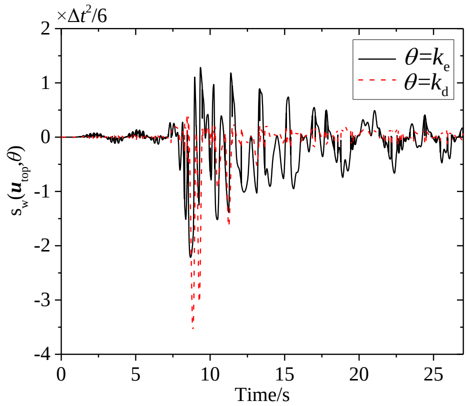

(a) Parameters k_e and k_d

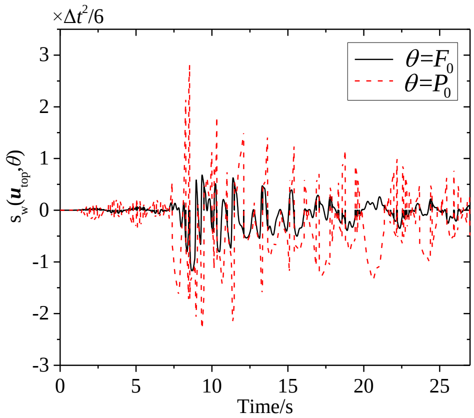

(b) Parameters F_0 and P_0

Fig. 8 Normalized response sensitivities of the roof displacement to the adjacent brace parameters

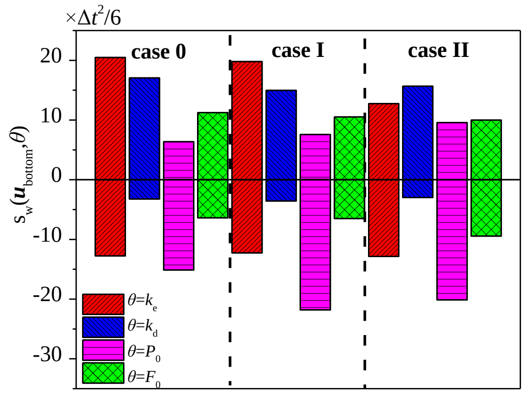

Fig. 9 Maximum and minimum normalized sensitivities of the first floor displacement to the considered parameters

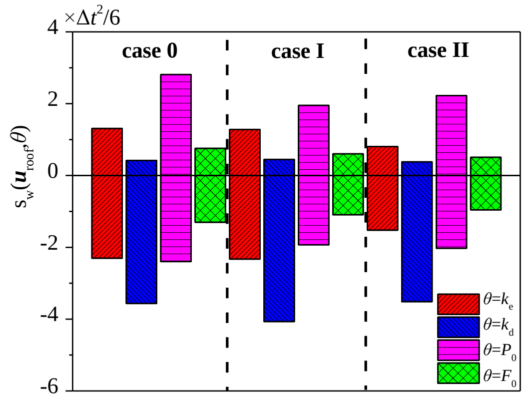

Fig. 10 Maximum and minimum normalized sensitivities of the roof displacement to the considered parameters

speculated that the parameter sensitivity distribution is quite discrepant along the height. It is also observed that the parameter P_0 always shows an opposite extreme effect on the displacement response compared to other brace parameters. The influence of parameter F_0 on the structural seismic behavior is relatively small, as the linear dynamic analysis may ignore the positive effect of the additional energy dissipation caused by the resistance to structural damage evolution, while the contribution of other parameters to the stiffness matrix is quite obvious. Case I magnifies the greatest influence of P_0 at the first floor and k_d in the roof on the responses, and case II minifies the influence of k_e which is a critical parameter for the natural vibration characteristics and the structure responses around the equilibrium position.

4.4 Sensitivity-based GA optimization analysis

Note that the original structure, brace-structure with default brace parameters, and brace-structure with brace parameter optimization in Case 0, case I and case II are respectively denoted as SYS-O, SYS-D, SYS-Case 0, SYS-Case I and SYS-Case II. Figs. 11-15 show the dynamic responses of the structure due to the 1999 Kocaeli earthquake. The responses are examined in terms of the roof displacement u_{roof}, absolute acceleration $\ddot{u}_{roof}$ and inter-story drift ratio.

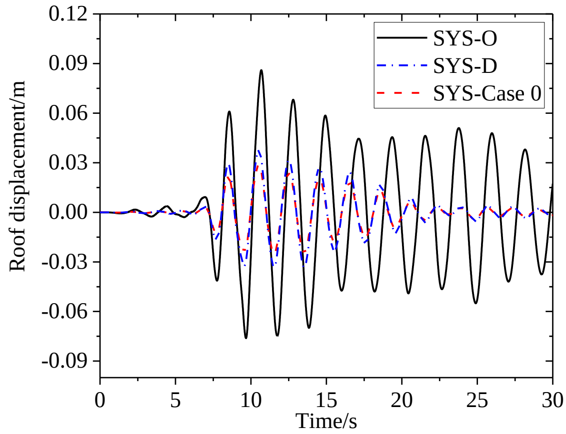

Fig. 11 Roof displacements time history of SYS-O, SYS-D and SYS-Case 0

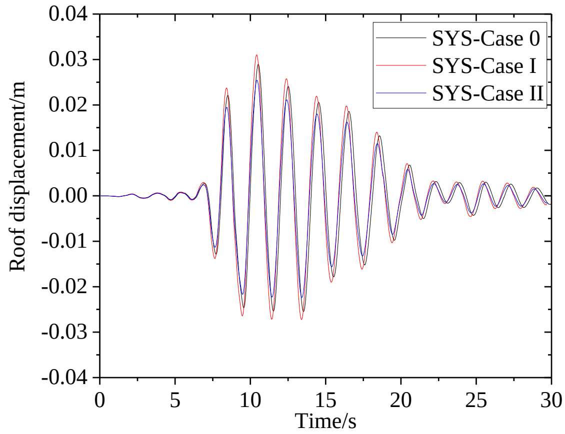

Fig. 12 Roof displacements time history of SYS-Case 0, SYS-Case I and SYS-Case II

The improvement of the maximum roof displacements from SYS-O to SYS-Case 0 is 66.3%, and the responses are minimized by more than 80% after the time when extreme value occurs. The response of SYS-Case 0 has certain reduction compared to that of SYS-D. The roof displacements of SYS-Case 0, SYS-Case I and SYS-Case II begin to show difference after the 7th second, and SYS-Case II shows better seismic performance than SYS-Case 0 does. The acceleration amplifications occur in this brace-structure system. The roof displacement is effectively improved, despite the adverse effect during the minor shock and the acceleration amplification due to the increase of the initial structural stiffness.

The inter-story drift ratio envelop is a significant performance index closely related to the component damage during the earthquake. The maximum drift ratio of SYS-Case 0 is decreased by 68% compared to SYS-O, while the maximum drift ratio of SYS-D is decreased by 60%. The distribution of maximum drift ratio in SYS-Case 0 is more uniform as well, as shown in Fig. 14. It seems that SYS-Case I is adversely affected by the strategy that amplifies the change rate of parameters with large sensitivity, leading to the worst optimization in these three cases. The results in Fig. 15 show that optimization in SYS-case II makes it possible for a better seismic performance than those of both

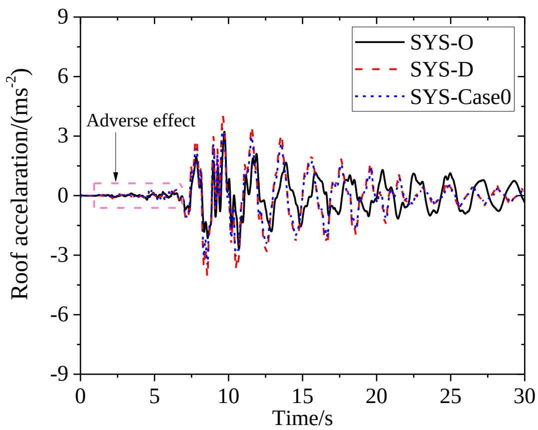

Fig. 13 Roof accelerations time history of SYS-O, SYS-D and SYS-Case 0

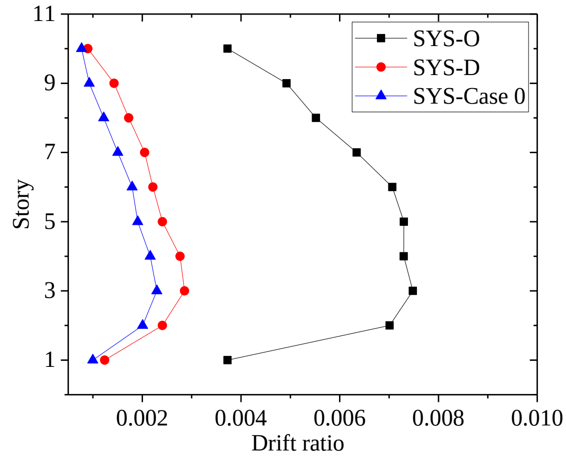

Fig. 14 Inter-story drift ratio envelopes of SYS-O, SYS-D and SYS-Case 0

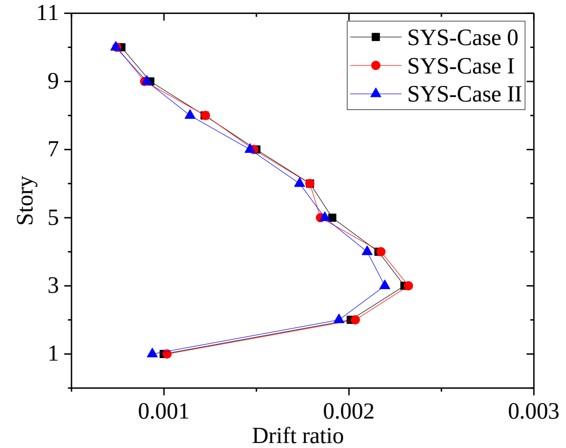

Fig. 15 Inter-story drift ratio envelopes of SYS-Case 0, SYS-Case I and SYS-Case II

Table 2 Maximum absolute values of response quantity in 5 different systems

Response	SYS-O	SYS-D	SYS-Case 0	SYS-Case I	SYS-Case II
u_{roof}/mm	86.02	38.05	28.94	31.02	25.45
$\ddot{u}_{roof}$ /ms^{-2}	3.22	4.10	3.51	3.78	3.73
Drift ratio	0.00718	0.00286	0.00230	0.00232	0.00219

Table 3 Optimal parameters of PS-SCED brace in SYS-Case 0

Story	k_e/(kN·m^{-1})	k_d/(kN·m^{-1})	d_0/m	P_0/N	F_0/N	β	γ
1	11532.2	1076.9	0.00200	9841.7	10934.6	-4.993	5.993
2	9918.1	1011.9	0.00208	10584.7	9624.5	-5.408	6.408
3	11035.4	980.1	0.00201	9571.7	10438	-6.210	7.210
4	12297.1	1003.2	0.00178	10712.4	10780	-4.994	5.994
5	9010.3	1055.4	0.00235	10073.5	10446.6	-4.895	5.895
6	8987.8	1043.4	0.00218	9427.8	10524.4	-5.676	6.676
7	9301.8	998.4	0.00220	9399.5	10182	-4.891	5.891
8	9946.2	1020	0.00208	10458.6	10067.5	-4.750	5.750
9	10877.1	1061.6	0.00172	8982.4	9529.3	-5.736	6.736
10	10562	989.1	0.00196	10156.4	10087.9	-5.045	6.045
Average	10215.1	1018.1	0.00204	9920.9	10261.5	-5.260	6.260

SYS-Case 0 and SYS-Case I. The maximum absolute values of response quantities are shown in Table 2 to help illustrate the difference of seismic behaviors among these 5 systems. Even the roof acceleration is not considered as the objective function during the optimization, it is obviously controlled after GA optimization as well.

The typical hysteretic responses of PS-SCED braces in SYS-Case II are shown in Fig. 16. The braces in the second and third stories represent two types of the relationship of the friction force and pre-pressed force (P_0>F_0 and P_0<F_0). For braces with different friction forces and pre-pressed forces, they exhibit stable and repeatable flag-shaped hysteretic responses, and their residual deformations are effectively reduced. The maximum displacement of the braces in the second and third stories are 267.5% and 325.5% of the activation displacement, respectively, indicating that the braces provide sufficient energy dissipation and stiffness after activation. Generally, the energy dissipation devices in the structure cannot reduce the residual deformation, and the residual deformation ratio of the structure after earthquakes is close to the inter-story drift ratio during earthquakes. However, in SYS-Case II, the residual displacements of the braces in the second and third stories are 12.3% and 33.0% of the maximum displacement, respectively, indicating that the braces can effectively reduce the residual deformation ratio of the structure.

The optimal parameters of PS-SCED brace in SYS-Case 0 are listed in Table 3, and the average value of each design parameter change does not exceed 5% of its initial parameter value. Figs. 17 and 18 show the comparisons of the visualized parameter changes in SYS-Case I and SYS-Case II with parameters normalized by the default values, respectively. Most optimal brace parameters in SYS-Case I seem to decrease after the GA based optimization, and the amplitude of parameter variations in SYS-Case II is much wider than that in SYS-Case I.

To study the impacts on the algorithm convergence and the GA operator by different ways of c_v correction, the evolutions of objective functions and generation numbers in SYS-Case 0, SYS-Case I and SYS-Case II are compared, as shown in Figs. 19 and 20. The objective function in SYS-Case I declines at the lowest speed. The fluctuation of the

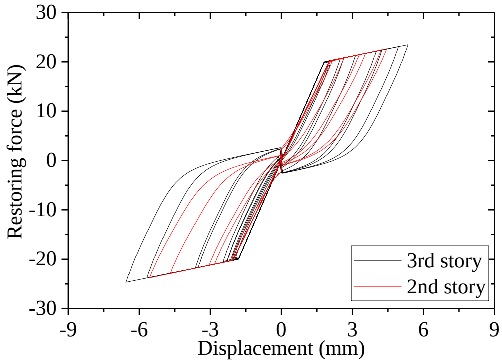

Fig. 16 Hysteretic curves of braces in SYS-Case II.

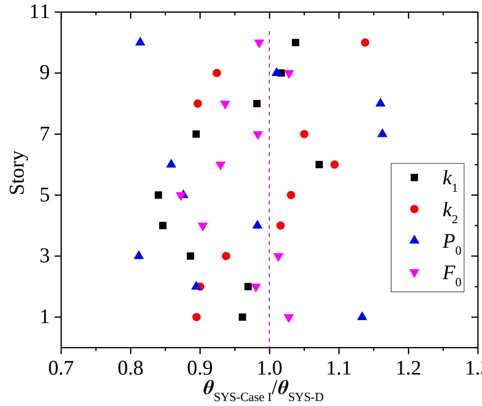

Fig. 17 Optimal brace parameters considered in SYS-Case I normalized by the default values

objective function curves in SYS-Case 0 is obviously greater than those in SYS-Case I and SYS-Case II, proving a better convergence of the optimization flow in SYS-Case I and SYS-Case II. For the smaller objective function, the optimization in SYS-Case II pays for more cycles of natural selection in GA. But a large number of generations do not mean a large amount of calculation. Because of the same restrain conditions, it is inevitable for the population size in different cases to become feeble and die. It can be observed that the population size curve of SYS-Case II declines at the fastest speed, and the attenuation speed of population of SYS-Case II is larger than that of SYS-Case 0. SYS-Case II only contains 11,978 times of dynamic solution even with a large number of generations, compared to the 14,163 times

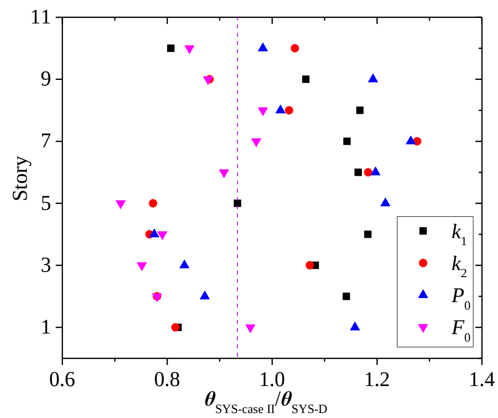

Fig. 18 Optimal brace parameters considered in SYS-Case II normalized by the default values

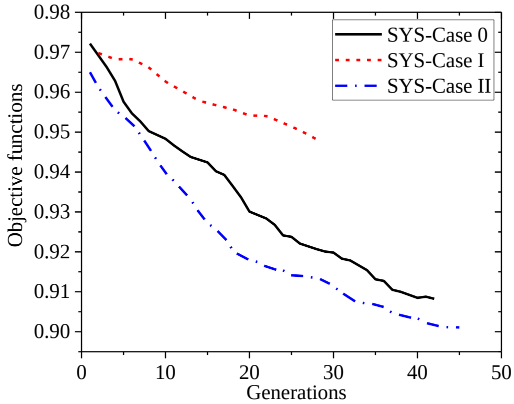

Fig. 19 Evolution of objective function in SYS-Case 0, SYS-Case I and SYS-Case II

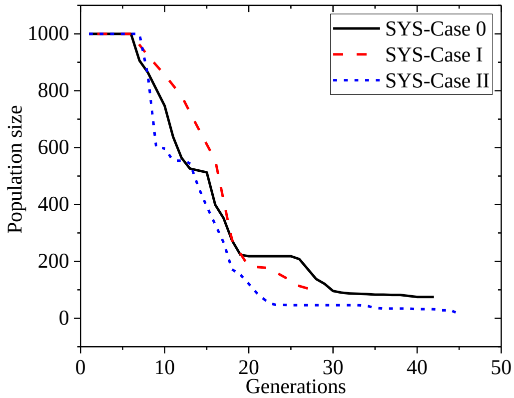

Fig. 20 Evolution of population size in SYS-Case 0, SYS-Case I and SYS-Case II

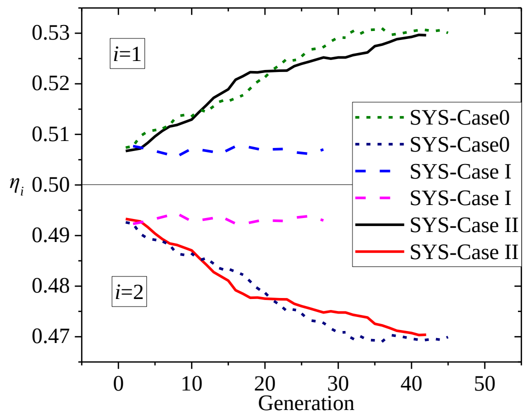

Fig. 21 Evolution of η_i in SYS-Case 0, SYS-Case I and SYS-Case II

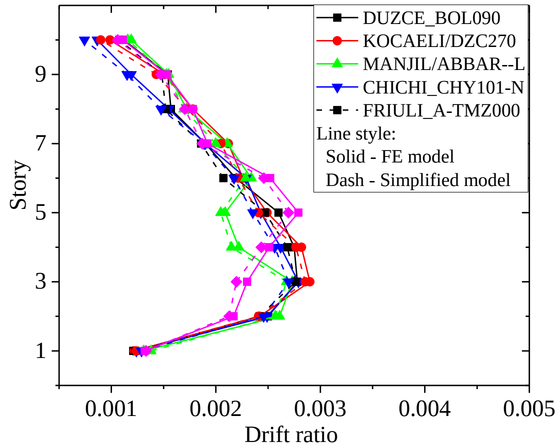

Fig. 22 Inter-story drift ratio envelopes of SYS-D obtained by FE and simplified models

of solution in SYS-Case 0. The accuracy and computational cost of GA optimization is contradictory. In order to improve the calculation accuracy, the size of initial population should be increased and the time integration interval Δt can be reduced. But this also leads to an increase in the computational cost. In practice, engineers can balance them according to calculation conditions. In this study, the size of initial population is 1000 and the time integration interval Δt is 0.01s.

To explain why the results of roof displacements are not as good as that of the inter-story drift ratio, the combination coefficient η_i in this multi-objective optimization problem is given in Fig. 21. η_1 in SYS-Case 0 and SYS-Case II which represent the proportion of drift ratio in the Eq.(13) are all more than 0.5 and continually increase as the number of generations increases. It certainly prompts the GA operator to select the individuals with smaller drift ratio instead of these with smaller roof displacement, because GA operator only conducts selections according to the objective function. In order to obtain a more balanced optimization results, a further study should be carried out towards the evolution of the combination coefficient η_i.

4.5 Accuracy of the simplified model analysis

The accuracy of the simplified model analysis is the basis for applying GA to optimize. Therefore, it is necessary to use the finite element (FE) model to check and verify the calculation results of the simplified model. Fig. 22 shows the inter-story drift ratio envelopes of SYS-D obtained by FE and simplified models due to 5 severest ground motions.

It can be seen that the inter-story drift ratios obtained by the simplified model is mostly slightly smaller than those obtained by the FE model analysis, and the relative errors are not more than 15%. The simplified model not only accurately represents the structural responses, but also greatly saves the computational cost. The automatic optimization design of the brace-structure can be realized through the docking of structural response results of the simplified model with the GA operator.

In future works, a mixed explicit-implicit time integration approach (Greco *et al.* 2018, Vaiana *et al.* 2018) can be used to drastically reduce the computational effort of the nonlinear time history analysis.

5. Conclusions

In this paper, a piecewise modified mechanical model with two state variables of PS-SCED brace is proposed to avoid the distortion due to the random seismic inputs. The formulation of the MDOF systems equipped with the braces is established in an incremental form of linear acceleration method. The accuracy of the simplified model is verified by the calculation results of FE model. A GA based PS-SCED brace optimization with multi-objective functions is developed to obtain the optimal solutions from the primary design parameters. Meanwhile, the structural response sensitivities with respect to the brace parameters are derived based on direct differentiation method, which is implemented into the GA operator for the parameter change rates correction in two opposite cases.

Due to the severest ground motion, the normalized sensitivity analysis indicates that the parameters k_e and P_0 show dominant effects on the node displacements before the braces start to work. Moreover, the pre-pressed force P_0 always shows an opposite extreme value effect on the displacement responses compared to other brace parameters, and the influence of the damping force F_0 on the structural seismic behavior is always in a relatively low level. Case I magnifies the greatest influence of P_0 at the first floor and k_d in the roof on the response while case II minifies the influence of k_e. During the middle and later periods of the earthquake, the roof displacements improve a lot in SYS-Case 0, SYS-Case I and SYS-Case II with no obvious distinctions. These three systems all reduce the maximum drift ratio of the structure, nonetheless, SYS-Case II stands out with a better distribution of inter-story deformation and a drift ratio reduction. The average of each parameter change after the optimization does not exceed 5% of the initial parameters, resulting in few construction cost alteration. The brace parameter dispersion in SYS-Case II remains the biggest, and the corresponding computational convergence is the best with a moderate rate of decay in population size. Although SYS-Case I has the lowest calculation cost, its optimization result is actually the worst. Both the combination coefficients η_1 in SYS-Case 0 and SYS-Case II are more than 0.5 all the time, leading to an unbalanced selection in GA operator.

Obviously, it is applicable to choose SYS-Case II as the optimized object when the operational capability is sufficient enough. We acknowledge that the results correspond to linear dynamic analyses only, so further researches should consider the nonlinear cases, such as the collapse performance, and other deformational structures, such as core-tube and frame-shear walls. Besides, it is necessary to find a stable way of selection in GA operator for certain engineering performance requirements.

Acknowledgments

The research described in this paper was financially supported by the National Natural Science Foundation of China [grant numbers 51578058]; and Beijing Natural Science Foundation of China [grant numbers 8172038].

References

Abbasnia, R., Shayanfar, M. and Khodam, A. (2014), “Reliability-based design optimization of structural systems using a hybrid genetic algorithm”, *Struct. Eng. Mech.*, **52**(6), 1099-1120. https://doi.org/10.12989/sem.2014.52.6.1099.

Chou, C.C. and Chung, P.T. (2014), “Development and seismic tests of a cross-anchored dual-core self-centering brace using steel tendons as tensioning elements”, *Proceedings of the 10th National Conference on Earthquake Engineering*, Anchorage, USA.

Dede, T. and Ayvaz, Y. (2013), “Structural optimization with teaching-learning-based optimization algorithm”, *Struct. Eng. Mech.*, **47**(4), 495-511. http://dx.doi.org/10.12989/sem.2013.47.4.495.

Degertekin, S.O. and Hayalioglu, M.S. (2010), “Harmony search algorithm for minimum cost design of steel frames with semi-rigid connections and column bases”, *Struct. Multidiscip. O.*, **42**(5), 755-768. https://doi.org/10.1016/j.compstruc.2005.02.009.

Ebrahimian, H., Jalayer, F., Lucchini, A., Mollaioli, F. and Manfredi, G. (2015), “Preliminary ranking of alternative scalar and vector intensity measures of ground shaking”, *B. Earthq. Eng.*, **13**(10), 2805-2840. https://doi.org/10.1007/s10518-015-9755-9.

Erochko, J., Christopoulos, C., Tremblay, R. and Kim, H.J. (2013), “Shake table testing and numerical simulation of a self-centering energy dissipative braced frame”, *Earthq. Eng. Struct. Dynam.*, **42**(11), 1617-1635. https://doi.org/10.1002/eqe.2290.

FEMA P695 (2009), Quantification of building seismic performance factors, Federal Emergency Management Agency; Washington, D.C., USA.

GB50011-2010 (2016), Code for seismic design of buildings, Ministry of Housing and Urban-Rural Development; Beijing, China.

Greco, F., Luciano, R., Serino, G. and Vaiana, N. (2018), “A mixed explicit-implicit time integration approach for nonlinear analysis of base-isolated structures”, *Ann. Solid Struct. Mech.*, **10**: 17-29. https://doi.org/10.1007/s12356-017-0051-z.

Gu, Q., Zona, A., Peng, Y. and Dall’Asta, A. (2014), “Effect of buckling-restrained brace model parameters on seismic structural response”, *J. Constr. Steel Res.*, **98**(7), 100-113. https://doi.org/10.1016/j.jcsr.2014.02.009.

Guerrini, G., Restrepo, J.I., Massari, M. and Vervelidis, A. (2014), “Seismic behavior of posttensioned self-centering precast concrete dual-shell steel columns”, *J. Struct. Eng.*, **141**(4), https://doi.org/10.1061/(ASCE)ST.1943-541X.0001054.

Henry, R.S., Sritharan, S. and Ingham, J.M. (2016), “Finite element analysis of the PreWEC self-centering concrete wall system”, *Eng. Struct.*, **115**, 28-41. https://doi.org/10.1016/j.engstruct.2016.02.029.

Ismail, M., Ikhouane, F. and Rodellar, J. (2009), “The hysteresis Bouc-Wen model, a survey”, *Arch. Comput. Methods Eng.*, **16**(2), 161-188. https://doi.org/10.1007/s11831-009-9031-8.

Kiani, J. and Pezeshk, S. (2017), “Sensitivity analysis of the seismic demands of RC moment resisting frames to different aspects of ground motions”, *Earthq. Eng. Struct. Dynam.*, **46**(15), 2739-2755. https://doi.org/10.1002/eqe.2928.

Liu, M., Burns, S.A. and Wen, Y.K. (2010), “Optimal seismic design of steel frame buildings based on life cycle cost

considerations", *Earthq Eng Struct Dynam*, **32**(9), 1313-1332. https://doi.org/10.1002/eqe.273.
Losanno, D., Londono, J.M., Zinno, S. and Serino, G. (2017a), "Effective damping and frequencies of viscous damper braced structures considering the supports flexibility", *Comput. Struct.*, **207**, 121-131. https://doi.org/10.1016/j.compstruc.2017.07.022.
Losanno, D., Spizzuoco, M. and Serino, G. (2014), "Optimal design of the seismic protection system for isolated bridges", *Earthq. Struct.*, **7**(6), 969-999. http://dx.doi.org/10.12989/eas.2014.7.6.969.
Losanno, D., Spizzuoco, M. and Serino, G. (2015), "An optimal design procedure for a simple frame equipped with elastic-deformable dissipative braces", *Eng. Struct.*, **101**, 677-697. https://doi.org/10.1016/j.engstruct.2015.07.055.
Losanno, D., Spizzuoco, M. and Serino, G. (2017b), "Design and retrofit of multi-story frames with elastic-deformable viscous damping braces", *J. Earthq. Eng.*, **2017**, 1-24. https://doi.org/10.1080/13632469.2017.1387193.
Marshall, J.D. and Charney, F.A. (2012), "Seismic response of steel frame structures with hybrid passive control systems", *Earthq. Eng. Struct. Dynam.*, **41**(4), 715-733. https://doi.org/10.1002/eqe.1153.
McCormick, J., Aburan, H., Ikenaga, M. and Nakashima, M. (2008), "Permissible residual deformation levels for building structures considering both safety and human elements", *Proceedings of the 14th World Conference on Earthquake Engineering*, Beijing, China, October.
Rojas, P., Caballero, M., Ricles, J.M. and Sause, R. (2009), "Plastic limit analysis of self-centering steel moment resisting frames", *Proceedings of 6th International Conference on Behaviour of Steel Structures in Seismic Areas*, Philadelphia, USA, August.
Rojas, H.A., Foley, C. and Pezeshk, S. (2011), "Risk-based seismic design for optimal structural and nonstructural system performance", *Earthq. Spectra*, **27**(3), 857-880. https://doi.org/10.1193/1.3609877.
Vaiana, N., Sessa, S., Marmo, F. and Rosati, L. (2018), "A class of uniaxial phenomenological models for simulating hysteretic phenomena in rate-independent mechanical systems and materials", *Nonlinear Dynam.*, **93**(3): 1647-1669. https://doi.org/10.1007/s11071-018-4282-2.
Wang, W., Fang, C. and Liu, J. (2017), "Self-centering beam-to-column connections with combined superelastic SMA bolts and steel angels", *J. Struct. Eng.*, **143**(2), 04016175. https://doi.org/10.1061/(ASCE)ST.1943-541X.0001675.
Xu, H.J., Ding, Z.H., Lu, Z.R. and Liu, J.K. (2015), "Structural damage detection based on Chaotic Artificial Bee Colony algorithm", *Struct. Eng. Mech.*, **55**(6), 1223-1239. http://dx.doi.org/10.12989/sem.2015.55.6.1223.
Xu, X., Zhang, Y.F. and Luo, Y.Z. (2016a), "Self-centering modularized link beams with post-tensioned shape memory ally rods", *Eng. Struct.*, **112**, 47-59. https://doi.org/10.1016/j.engstruct.2016.01.006.
Xu, L.H., Fan, X.W. and Li, Z.X. (2016b), "Development and experimental verification of a pre-pressed spring self-centering energy dissipation brace", *Eng. Struct.*, **127**, 49-61. https://doi.org/10.1016/j.engstruct.2016.08.043.
Xu, L.H., Fan, X.W. and Li, Z.X. (2016c), "Cyclic behavior and failure mechanism of self-centering energy dissipation braces with pre-pressed combination disc springs", *Earthq. Eng. Struct. Dynam.*, **46**(7), 1065-1080. https://doi.org/10.1002/eqe.2844.
Xu, L.H., Xie, X.S., and Li, Z.X. (2018a), "Development and experimental study of a self-centering variable damping energy dissipation brace", *Eng. Struct.*, **160**, 270-280. https://doi.org/10.1016/j.engstruct.2018.01.051.
Xu, L.H., Xie, X.S., and Li, Z.X. (2018b), "A self-centering brace with superior energy dissipation capability: development and experimental study", *Smart Mater. Struct.*, **27**(9), 095017.
Yi, T.H., Zhou, G.D., Li, H.N. and Zhang, X.D. (2015), "Optimal sensor placement for health monitoring of high-rise structure based on collaborative-climb monkey algorithm", *Struct. Eng. Mech.*, **54**(2), 305-317. http://dx.doi.org/10.12989/sem.2015.54.2.305.
Yurdakul, Ö. and Avsar, Ö. (2016), "Strengthening of substandard reinforced concrete beam-column joints by external post-tension rods", *Eng. Struct.*, **107**, 9-22. https://doi.org/10.1016/j.engstruct.2015.11.004.
Zhang, A.L., Zhang, Y.X., Li, R. and Wang, Z.Y. (2016), "Cyclic behavior of a prefabricated self-centering beam-column connection with a bolted web friction device", *Eng. Struct.*, **111**, 185-198. https://doi.org/10.1016/j.engstruct.2015.12.025.

CC